2013-03

Optical attenuation coefficient in individual ZnO nanowires

Little, Anree

Optical attenuation coefficient in individual ZnO nanowires

Anree Little, Abigail Hoffman, and Nancy M. Haegel*

Department of Physics, Naval Postgraduate School, Monterey, California 93943 USA
*UUnmhaegel@nps.eduUU

Abstract: Attenuation coefficient measurements for the propagation of bandedge luminescence are made on individual ZnO nanowires by combining the localized excitation capability of a scanning electron microscope (SEM) with near-field scanning optical microscopy (NSOM) to record the distribution and intensity of wave-guided emission. Measurements were made for individual nanostructures with triangular cross-sections ranging in diameter from 680 to 2300 nm. The effective attenuation coefficient shows an inverse dependence on nanowire diameter (d^{-1}), indicating scattering losses due to non-ideal waveguiding behavior.

OCIS codes: (160.4236) Nanomaterials; (130.5990) Semiconductors; (180.4243) Near-field microscopy; (250.1500) Cathodoluminescence; (290.0290) Scattering.

References and links

1. R. Könenkamp, R. C. Word, and C. Schlegel, "Vertical nanowire light-emitting diode," Appl. Phys. Lett. **85**(24), 6004–6006 (2004).
2. J. Bao, M. A. Zimmler, F. Capasso, X. Wang, and Z. F. Ren, "Broadband ZnO single-nanowire light-emitting diode," Nano Lett. **6**(8), 1719–1722 (2006).
3. M. H. Huang, S. Mao, H. Feick, H. Yan, Y. Wu, H. Kind, E. Weber, R. Russo, and P. Yang, "Room-temperature ultraviolet nanowire nanolasers," Science **292**(5523), 1897–1899 (2001).
4. M. A. Zimmler, J. Bao, F. Capasso, S. Muller, and C. Ronning, "Laser action in nanowires: observation of the transition from amplified spontaneous emission to laser oscillation," Appl. Phys. Lett. **93**(5), 051101 (2008).
5. P. J. Pauzauskie and P. Yang, "Nanowire photonics," Mater. Today **9**(10), 36–45 (2006).
6. M. Willander, O. Nur, Q. X. Zhao, L. L. Yang, M. Lorenz, B. Q. Cao, J. Zúñiga Pérez, C. Czekalla, G. Zimmermann, M. Grundmann, A. Bakin, A. Behrends, M. Al-Suleiman, A. El-Shaer, A. Che Mofor, B. Postels, A. Waag, N. Boukos, A. Travlos, H. S. Kwack, J. Guinard, and D. Le Si Dang, "Zinc oxide nanorod based photonic devices: recent progress in growth, light emitting diodes and lasers," Nanotechnology **20**(33), 332001 (2009).
7. Z. L. Wang, "Zinc oxide nanostructures: growth, properties and applications," J. Phys. Condens. Matter **16**(25), R829–R858 (2004).
8. X. Wang, J. Song, and Z. L. Wang, "Single crystal nanocastles of ZnO," Chem. Phys. Lett. **424**(1-3), 86–90 (2006).
9. M. Law, D. J. Sirbuly, J. C. Johnson, J. Goldberger, R. J. Saykally, and P. Yang, "Nanoribbon waveguides for subwavelength photonics integration," Science **305**(5688), 1269–1273 (2004).
10. X. D. Wang, J. H. Song, and Z. L. Wang, "Nanowire and nanobelt arrays of zinc oxide from synthesis to properties and to novel devices," J. Mater. Chem. **17**(8), 711–720 (2007).
11. N. M. Haegel, D. J. Chisholm, and R. A. Cole, "Imaging transport in nanowires using near-field detection of light," J. Cryst. Growth **352**(1), 218–223 (2012).
12. N. M. Haegel, T. J. Mills, M. Talmadge, C. Scandrett, C. L. Frenzen, H. Yoon, C. M. Fetzer, and R. R. King, "Direct imaging of anisotropic minority-carrier diffusion in ordered GaInP," J. Appl. Phys. **105**(2), 023711 (2009).
13. L. Baird, C. P. Ong, R. A. Cole, N. M. Haegel, A. A. Talin, Q. Li, and G. T. Wang, "Transport imaging for contact-free measurements of minority carrier diffusion in GaN, GaN/AlGaN and GaN/InGaN core-shell nanowires," Appl. Phys. Lett. **98**(13), 132104 (2011).
14. Y. S. Park and J. R. Schneider, "Index of refraction of ZnO," J. Appl. Phys. **39**(7), 3049–3052 (1968).
15. A. M. Schwartzberg, S. Aloni, T. Kuykendall, P. J. Schuck, and J. J. Urban, "Optical cavity characterization in nanowires via self-generated broad-band emission," Opt. Express **19**(9), 8903–8911 (2011).
16. Q. Li, K. R. Westlake, M. H. Crawford, S. R. Lee, D. D. Koleske, J. J. Figiel, K. C. Cross, S. Fathololoumi, Z. Mi, and G. T. Wang, "Optical performance of top-down fabricated InGaN/GaN nanorod light emitting diode arrays," Opt. Express **19**(25), 25528–25534 (2011).
17. M. A. Zimmler, F. Capasso, S. Muller, and C. Ronning, "Optically pumped nanowire lasers: invited review," Semicond. Sci. Technol. **25**(2), 024001 (2010).

#179943 - $15.00 USD Received 16 Nov 2012; revised 15 Dec 2012; accepted 17 Dec 2012; published 6 Mar 2013

1. Introduction

One dimensional nanostructures, generally referred to as nanowires or nanorods, are of potential interest for light emitting diodes (LED) and lasers, since high packing density and dimensionally controlled growth resulting in dislocation free material may impact next-generation photon sources. The use of nanowires, whether for lasers, LEDs or more broadband sources, could have impact in areas that would benefit from lower cost "bottom up" fabrication, more compact sources or direct integration of photonic and electronic structures at the nanoscale. Nanowires are natural waveguides, due to their geometry and relatively high index of refraction. Both LED operation [1,2] and lasing behavior [3,4] have been demonstrated in ZnO nanowires and extensive research activity is on-going [5,6].

The one-dimensional structure of nanowires or nanorods provides both waveguiding and cavity confinement. In ZnO, nanowire growth is generally along the [0001] direction. Cross sectional areas are commonly hexagonal, but a wide range of geometries, depending on growth conditions, have been reported, including triangular cross sections [7,8]. Waveguiding has been studied in some detail [9]. Similarly important, however is scattering and absorption behavior, since it will always be the balance between emission efficiency (or gain for laser structures) and attenuation losses that will determine LED efficiency or lasing threshold. However, direct measures of absorption and attenuation in individual nanowires are extremely difficult due to the challenge of coupling an optical source to a single nanowire.

We present a method of making optical attenuation measurements in individual ZnO nanostructures that utilizes a combination of a scanning electron microscope for localized generation of light and a near-field scanning optical microscope for direct measure of the waveguided output. We investigate attenuation behavior as a function of nanowire diameter.

2. Samples and experimental approach

The materials of interest are ZnO nanostructures grown by physical vapor deposition [10]. After sublimation and growth on an alumina substrate, the wires were sonicated into solution and then dispersed horizontally on Si substrates. An SEM image of a collection of the structures and an "end-on" image of a representative wire are shown in Fig. 1. Because of their uniform cross section, triangular nanostructures were chosen for this study. Cross sectional dimensions along the base of the structure vary from several hundred nanometers to several microns.

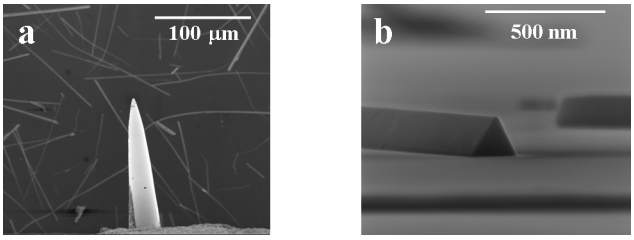

Fig. 1. ZnO nanowires dispersed horizontally on Si substrate, a) imaged at low magnification (1000X) in presence of NSOM fiber tip and b) cross sectional image of triangular nanowire at high magnification (260,000X).

The samples are placed in the SEM with a near-field scanning optical microscope integrated under the pole piece. This system, described in detail in [11], leverages the optical axis access of a Nanonics Multiview 2000 to enable combined AFM and NSOM in the presence of electron beam imaging of the sample. The system effectively combines three microscopes – 1) an SEM which is used in this case to locate and image individual nanowires and then to generate localized luminescence, 2) a tuning fork based AFM that maintains the system in the near-field and 3) an NSOM fiber to collect spatially resolved luminescence. This combination, which provides independent scanning capability for both the sample and the tip, allows for spatially resolved collection of luminescence that is generated at a point.

#179943 - $15.00 USD Received 16 Nov 2012; revised 15 Dec 2012; accepted 17 Dec 2012; published 6 Mar 2013

This is achieved by placing the SEM in "spot mode" operation at a fixed point on the sample and then scanning the NSOM probe. The resulting information can provide detailed information on waveguiding, as presented here, or can be used to optically determine, in a non-contact manner, the diffusion length of minority carriers [12,13].

Figure 2 shows a schematic of the experiment. The SEM beam is placed in spot mode at a measured distance from the end of the nanowire. The NSOM scan is done over a fixed region encompassing the end of the nanowire and the area beyond in order to image the waveguided luminescence emerging from the structure. Since the point of optical generation can be moved in a precise fashion along the nanowire, it is possible to measure the emitted intensity as a function of the distance that the light propagates in the nanowire.

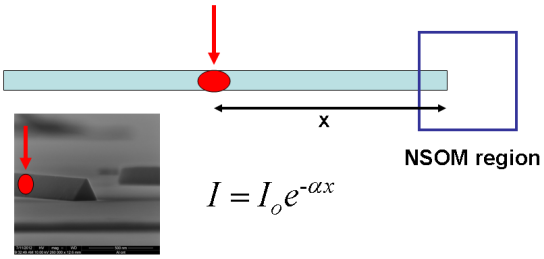

Fig. 2. Schematic of experimental approach illustrating electron beam incident on nanowire and area of NSOM scan.

The electron beam was operated at an accelerating voltage of 20 kV. This generates a spot size at the sample surface ranging from ~2 – 20 nm, depending on the current, but the incident electron energy is sufficient to create a generation volume that extends into the nanowire, localizing the generation volume to ~1 μm.

3. ZnO nanowire luminescence

Figure 3 shows a room temperature cathodoluminescence (CL) spectrum of the ZnO nanowires of interest. The luminescence was collected using a CL system with a parabolic collecting mirror and a ¼ m monochromator with a GaAs cooled PMT detector. As is common with many reports of luminescence from ZnO nanowires, we observe a peak near the bandedge at ~380 nm and then a broader, defect-related peak, which is relatively weak for these particular samples. For this work, filters were inserted into the optical path so that the luminescence measured by the NSOM scans is only the bandedge luminescence. Therefore, the attenuation coefficients reported here are for ultraviolet light over the range of ~370 to 410 nm, with a maximum at 380 nm. No indication of lasing behavior, as evidenced by the appearance of sharper optical transitions, was observed in CL measurements with increasing excitation over the range of excitation used in this work. We focus therefore on isotropically emitted spontaneous emission.

4. Experimental results

For a given nanowire, the wire was located in the SEM using standard imaging techniques. Then the SEM was operated in "spot mode," with the beam placed at a measured

#179943 - $15.00 USD Received 16 Nov 2012; revised 15 Dec 2012; accepted 17 Dec 2012; published 6 Mar 2013

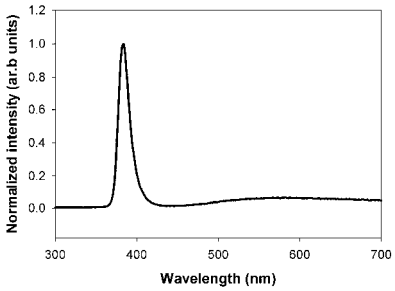

Fig. 3. 300 K luminescence

distance from the wire's end, as previously illustrated in Fig. 2. An NSOM image was then obtained from a region that captured the optical emission at the end of the wire. An example of the results, with the NSOM image superimposed on the AFM topography of the wire, is shown in Fig. 4 for a series of three excitation positions on a wire with a diameter of 1.0 μm. The wire diameter is measured by SEM, rather than the AFM topography, because the AFM convolutes the wire diameter with the diameter of the NSOM probe, which is at least 300 nm in diameter in this case. Fully resolved topography would require an AFM probe tip. The end of this particular wire was non-uniform, resulting in the particular spread pattern observed in the light emission.

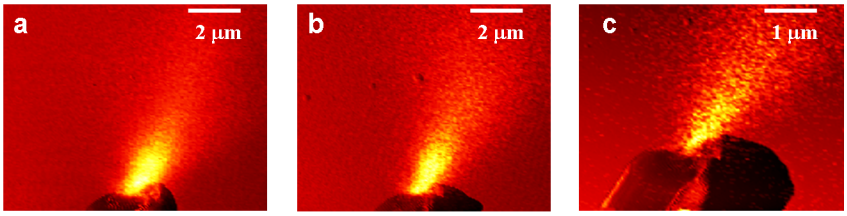

Fig. 4. NSOM image of light emitted from nanowire, superimposed on AFM image showing physical end of the structure. Results are shown for point source excitation locations of A) 10 μm, B) 20 μm and C) 40 μm from the end of the wire.

NSOM images were collected as a function of excitation distance to the end of the wire. The peak intensity within the image was then determined to obtain a relative measure of the variation of emission intensity as a function of excitation position. Excitation conditions were kept constant. These measurements were performed on four different nanowires of varying diameter. The light emission pattern, which is determined by the detailed nature of the end of the structure as seen in Fig. 4, does not affect the measurements since only relative intensity changes were relevant for a given wire. The intensity, as a function of position, was plotted as shown in Fig. 5. Using Beer's law

$$I = I_0 \exp(-\alpha x), \tag{1}$$

an effective attenuation coefficient was obtained for each wire.

The measured attenuation coefficients for the propagation of bandedge light increase with decreasing nanowire diameter. The size of these structures is such that 1) there are no quantum confinement effects involved, 2) the electron beam should generate electron-hole pairs throughout the full depth of the nanowire and result in photons initially propagating in all directions and 3) multimode propagation behavior should be expected in the waveguides. The third assumption is supported by calculating the diameter limit for single mode propagation. Using the estimate for the single mode cut off for a circular waveguide ($V < 2.405$ where V is the normalized frequency, $V = (2\pi aNA/\lambda)$ where a is the fiber radius, NA is the numerical aperture and λ is the wavelength), we obtain a maximum diameter of ~127 nm

#179943 - $15.00 USD Received 16 Nov 2012; revised 15 Dec 2012; accepted 17 Dec 2012; published 6 Mar 2013

for single mode propagation, using λ = 380 nm and a refractive index for ZnO of 2.5 [14]. The diameters for all structures measured here are significantly larger than this cut-off limit.

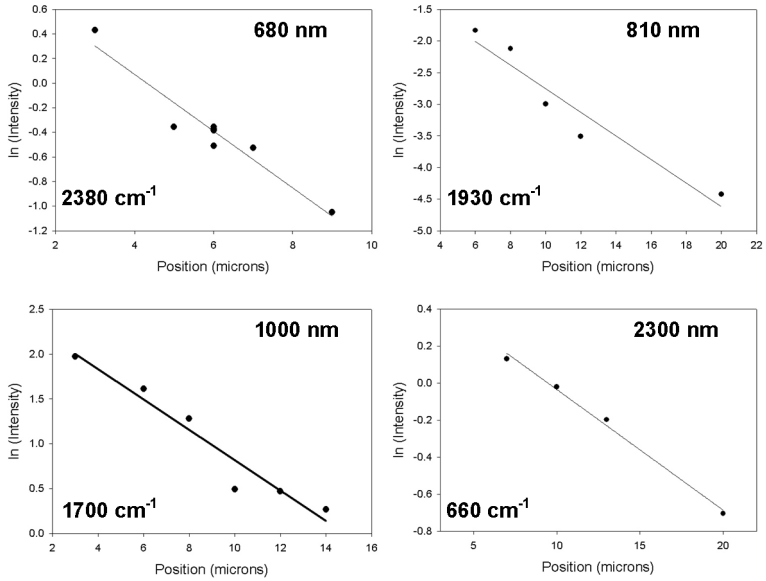

Fig. 5. Maximum intensity in NSOM images at the end of the wire as a function of the distance from the excitation point. The number in the upper right corner is the diameter of the nanostructure, to the nearest 10 nm. The lines represent a least squares fit to the data, with the resulting value for the attenuation coefficient given in the lower left corner.

With these conditions in mind, one hypothesis for the observed behavior is the increased frequency of reflections at the interfaces for off-axis modes propagating the length of the structure for smaller diameter waveguides. The nanostructures are not expected to be perfect waveguides, given their geometry and surface features, as well as effects associated with the presence of a substrate. We model, therefore, the dependence of the number of interactions with the interface (i.e., the number of bounces for a given off-axis mode per unit length) as a function of waveguide diameter and compare it to the measured diameter dependence for α.

If we consider an off-axis ray propagating down a high index waveguide of diameter d, the range of allowed off-axis angles will range from a minimum of $\theta = 0$ (the on-axis mode) to a maximum of $\theta = (90 - \theta_c)$, where θ is the angle from the center axis and θ_c is the critical angle for internal reflection. Simple geometry shows that $\tan\theta = d/(2L)$, where L is a unit distance along the nanowire. The number of reflections per unit distance is then

$$\frac{\#bounces}{unit\ length} = \frac{2}{4L} = \frac{2}{4\left(\frac{d}{2\tan\theta}\right)} = \frac{\tan\theta}{d}. \qquad (2)$$

The number of reflections at the surface per unit length, therefore, should be inversely proportional to the diameter of the wire. If we assume a fixed fractional loss per reflection, this would result in an attenuation coefficient which is also inversely proportional to diameter.

In Fig. 6, we plot the measured attenuation coefficients as a function of nanowire diameter to determine the power law. The line represents a least squares regression fit to the data, with a resulting slope of −1.05, an excellent match to the predicted dependence of d^{-1} for loss associated with attenuation effects associated with reflections at the surface.

#179943 - $15.00 USD Received 16 Nov 2012; revised 15 Dec 2012; accepted 17 Dec 2012; published 6 Mar 2013

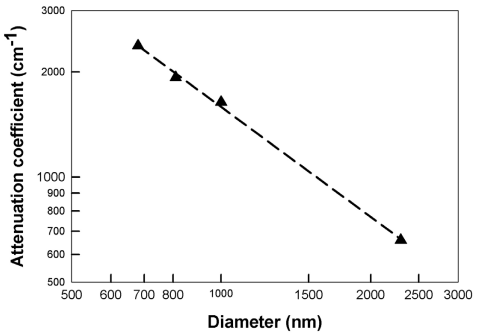

Fig. 6. Attenuation coefficient as a function of diameter. Dashed line shows a least squares fit with all data equally weighted, indicating $d^{-1.05}$ dependence.

The increase in attenuation coefficient with decreasing nanowire diameter is consistent with other reports suggesting that larger diameter nanowires or nanorods are higher efficiency waveguides. In particular, Schwartzberg et. al., studied GaN nanowires of dimensions ranging from 50 to 600 nm in diameter and reported that "below 100 nm in width, little waveguiding is observed." [15]. Li et. al. [16] found that InGaN/GaN nanoLEDs with diameter of ~200 nm did not reach efficiencies exceeding those of planar LEDs despite having lower dislocation densities and reduced piezoelectric polarizations. They attribute this primarily to heating effects or non-radiative recombination, but attenuation behavior and surface loss could also play some role. Finally, Zimmler et. al. [17], in a 2010 review of optically pumped nanowire lasers, present data on lasing of ZnO structures of various diameter that shows that structures with diameter below ~150-200 nm did not reach lasing threshold. Although this is explained primarily by modeling of the dependence of the reflection coefficient on diameter for the lower order lasing modes, it is interesting to note that decreased reflectivity for smaller diameters (which they believe lowers the cavity efficiency and inhibits lasing) would not be consistent with the loss of waveguiding in structures operating below threshold, as in Ref. 14. The very strong predicted loss of reflectivity for smaller diameters might be expected to mitigate to some extent the effects of increased surface recombination and encourage a net waveguide emission. It is possible, therefore, that increased scattering and loss effects with decreasing diameter, as have been shown here, may play a role in the overall performance both LED and laser structures investigated to date.

7. Conclusion

In summary, we have utilized a combination of a scanning electron microscope and a near field optical imaging system to measure the attenuation coefficient for waveguiding of bandedge luminescence in individual ZnO nanowires with cross sectional dimensions ranging from 680 to 2300 nm. The effective attenuation coefficient, associated with both absorption and scattering, varies inversely with nanostructure diameter, with a dimensional dependence of d^{-1}. This agrees with the expected behavior for attenuation that is dominated by scattering loss associated with reflection of off-axis light at the nanowire surface.

Acknowledgments

This work was supported by National Science Foundation Grant DMR-0804527. The ZnO nanostructures were provided by the group of Prof. Z. L. Wang at Georgia Institute of Technology. NMH acknowledges her status as a Senior Fulbright Fellow at Hebrew University during the preparation of this manuscript.

#179943 - $15.00 USD Received 16 Nov 2012; revised 15 Dec 2012; accepted 17 Dec 2012; published 6 Mar 2013